

## MODELING THE PAUZHETSKY GEOTHERMAL FIELD, KAMCHATKA, RUSSIA, USING iTOUGH2

A.V. Kiryukhin<sup>1</sup>, N.P. Asaulova<sup>2</sup>, S. Finsterle<sup>3</sup>, T.V. Rychkova<sup>1</sup>, and N.V. Obora<sup>2</sup>

<sup>1</sup>- Institute Volcanology and Seismology FEB RAS, Piip-9, P-Kamchatsky, Russia 683006

<sup>2</sup>- Kamchatskburgeotemia Enterprize, Krashenninnikova-1, Thermalny, Kamchatka, Russia, 684035

<sup>3</sup>- Lawrence Berkeley National Laboratory, MS-90-1116, One Cyclotron Rd, Berkeley, CA 94720, USA

e-mail: avk2@kscnet.ru

### **ABSTRACT**

The forward TOUGH2 modeling study of the Pauzhetsky geothermal field (Kiryukhin and Yampolsky, 2004) was followed by an iTOUGH2 analysis to obtain more reliable reservoir parameter estimations. The model was automatically calibrated against (1) natural state and (2) production data. For the natural state modeling, calibration data include 68 points (2 natural discharge rates, 14 reservoir pressures at -250 m.a.s.l., and 52 reservoir vertically averaged temperatures). The different quality of the calibration points was expressed by specifying appropriate standard deviations. Preliminary estimates of the principal parameters are: (1) permeability  $k = 87$  mD, and (2) an upflow rate  $Q_b = 40.5$  kg/s.

For the modeling of the exploitation phase, calibration data include 60 datasets: enthalpies of the exploitation wells (10 data sets), pressures in monitoring wells (24 data sets), and temperatures in monitoring wells (26 data sets), with a total of 15,030 calibration points. The following parameters are estimated: (1) reservoir compressibility, (2) reservoir fracture porosity, and (3) infiltration “window” permeabilities. Model calibration will be followed by an analysis of the sustainable capacity of the Pauzhetsky field.

### **INTRODUCTION**

The Pauzhetsky geothermal field has been developed since 1966, when a 5 MWe power plant was put into operation. The first reservoir engineering study of this field conducted by Sugrobov (1965) revealed a liquid-dominated reservoir with layer type tuffs at 170-190°C, with hot springs discharges at 31 kg/s. The lumped parameter model by Sugrobov (1976) yielded 460 kg/s lateral, high-temperature outflow from the Kambalny ridge into the geothermal reservoir. However, the initial 10 years of the exploitation at 160-190 kg/s show gradual temperature decline and chloride dilution of the production wells located near the natural discharge area, so new exploration wells were drilled, and exploitation gradually shifted away from the natural discharge area until temperatures of 200-220°C were

reached. Wells were drilled into a central upflow zone located 1.5-2.0 km southeast from the old production field (Yampolsky, 1976). The drop in temperatures and enthalpies continued, while total flow rate reached 220-260 kg/s between 1975 and 2005. The forward TOUGH2 modeling study of the field conducted by Kiryukhin and Yampolsky (2004) yielded the following estimates of the principal parameters: (1) An upflow rate of 220 kg/s with an enthalpy of 830-920 kJ/kg, (2) a permeability-thickness of 70 D·m in the central part of the field, and a compressibility of  $5.0 \cdot 10^{-7}$  Pa<sup>-1</sup>, (3) a fracture spacing of 162 m and fracture/matrix ratio of 0.1 for the dual-porosity model, and (4) the existence of constant pressure boundaries.

The sustainable capacity of the Pauzhetsky field became a critical question for power plant reconstruction and new binary technology implementation, and a more detailed calibration study was performed. In this study, iTOUGH2 was used for parameter estimation. The current numerical model (mesh has 424 elements, 294 being active) represents a 3-layer system (caprock, reservoir of 500-m thickness, base rock) with an interior upflow zone and external constant pressure recharge-discharge boundaries.

### **CONCEPTUAL HYDROGEOLOGICAL MODEL**

The Pauzhetsky geothermal field is situated inside the Pauzhetska volcano-tectonic depression (Fig.1). The oldest rocks penetrated by wells at 650-m depth are Miocene sandstones. Pauzhetska tuffs (N<sub>2</sub>-Q<sub>1</sub>) include welded tuffs, tuffaceous conglomerates, and psephitic tuffs. The caprock is represented by a 100-m thick layer of dacitic alevropelitic tuffs. Rhyolite and andesite-dacite extrusions (domes and ridges) of 0.01 to 8 km<sup>2</sup> size are common. The Dacite extrusion complex (Q<sub>2-3</sub>), which is located inside the 190°C zone, acts as a structural control for the temperature and permeability distribution. This complex is penetrated by wells 111, 124, 105, 101, 123, 107, 106, and 131 at depths more than 50 m. A graph of cumulative production rate per well vs. depth shows that most production occurs in the interval from 100 to 800 m depth, with a maximum rate of 23.2 kg/s.

This interval includes the lower and middle parts of the Pauzhetka tuff formation ( $N_2-Q_1$  pau<sub>1,2</sub>) and Golyginsky Layer ( $N_2$  gol). This is a clear indication of the layered structure of the permeability in the Pauzhetsky geothermal field. Integrated analysis of the field data shows the following reservoir characteristics:

(1) The Pauzhetsky reservoir is layered with an area of  $2 \times 2.5$  km<sup>2</sup> and an average penetrated thickness of 505 m connected at the bottom with the hot water upflow.

(2) Well logging analysis show a double-porosity response of the reservoir, with a fracture volume fraction (FV) of 0.28 and an average fracture spacing (FS) of 170 m.

(3) Natural thermal discharges include dominant hot boiling springs discharge with a measured rate of 31 kg/s, and steaming grounds (Verkhnee and East with a total discharge rate of 0.7 MWt).

(4) Permeability-thickness  $kM$  and total production zones compressibility  $C_r \phi M$  estimates based on multiwell flowtest semi-log analyses show a  $kM$  range from 35 to 94 D-m and  $C_r \phi M = 9.0 \cdot 10^{-6}$ . Laboratory testing of reservoir rock samples (matrix) show a porosity up to 0.2 and a density of 1500 – 1800 kg/m<sup>3</sup> (Ladygin et al., 2000), and an average heat conductivity (dry conditions) of 1.6 W/m °C (Sugrobov and Yanovsky 1987).

(5) Initial reservoir pressure is 34.5-35.5 bars at -250 m.a.s.l., and tends to increase in south-easterly direction (North site of the field).

(6) The production reservoir temperature is 180 – 220 °C; the upflow zone is delineated by a temperature contour within the drilled part of the field.

(7) The chemical composition of the thermal fluid is characterized by Cl-Na and CO<sub>2</sub>-N<sub>2</sub>, with a dissolved solids content of 2.7 – 3.4 g/kg. Hydroisotopic ( $\delta D$ ,  $\delta O_{18}$ ) composition of the thermal fluids correspond to the Kurile Lake water – Kamalny Ridge cold springs range, which demonstrates their meteoric origin.

Based on the above data, the following hydrogeological conceptual model was assumed. Cold meteoric water infiltrates through open fractures at 5-6 km depth in a high-temperature zone above 250°C (where remaining hot magma bodies are located), heats up and upflows. Upflows of high-temperature fluids with enthalpies of 950-1050 kJ/kg through the base and Miocene sandstone rocks to reach the volcanogenic-sedimentary basin, where layered production reservoir takes place (see Figure 1).

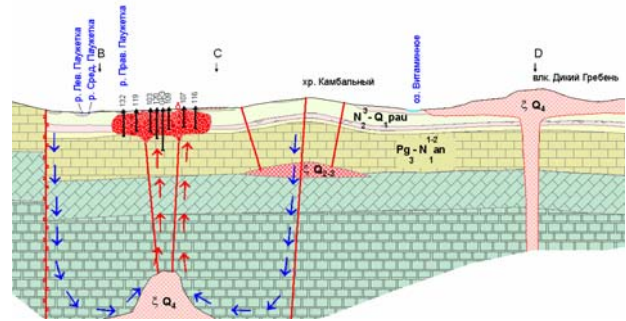


Figure 1. Conceptual model of the Pauzhetsky geothermal field.

## NUMERICAL MODEL SETUP

### Grid Generation

The geothermal reservoir was represented in the model as a three-layer system that covers the existing well field. This model includes: (1) a middle layer representing the hydrothermal reservoir at -250 m.a.s.l. with an average thickness of 500 m; (2) an upper layer caprock with “hydraulic windows” allowing for natural discharge (from the top of the hydrothermal reservoir at 0 m.a.s.l. to the land surface); and (3) a base layer hosted upflow plumbing system zone with an average thickness 500 m. The preprocessor A-mesh was used for grid generation. The total number of elements is 424, including 294 active elements (Fig.2-4).

### Boundary Conditions

Mass sources were introduced in the model where the natural high-temperature upflows were assumed to occur, with the enthalpies corresponding to the liquid water temperature in the range 950-1050 kJ/kg. Heat sources were assigned at the bottom of the model layer to reproduce background conductive heat flow (0.063 W/m<sup>2</sup>). Lateral no-flow boundaries were assigned. Discharge conditions were assigned through additional inactive elements CR1 1, C135 1, C 5, and C142 of the caprock “hydraulic window” with the centers at the land surface, constant atmospheric pressure, and 100°C discharge temperature. These elements were vertically connected to elements R 1, 135, 5 and 142 of the mid-layer hydrothermal reservoir, where most of the natural discharge occurs in form of hot springs. Additional natural discharge elements (CC27 / FF27) were used to represent hidden natural discharge zones revealed by Sugrobov (1965). Conductive heat loss from the hydrothermal reservoir to the caprock was modeled by specifying inactive boundary elements with a constant temperature of 5°C.

**Zonation and Rock Properties**

The model domain was subdivided into several zones to represent major discharge zones (referred to as “hydraulic windows” in the caprock, see Fig. 3). The mid-layer hydrothermal reservoir was subdivided into a central part (ROCK1), boundary parts (ROCK4), and an internal, relatively impermeable domain (ROCK2) (Fig. 2). The base layer was divided into the upflow zone (BASE2) and host rock (BASE1) (Fig. 4).

The caprock and hydrothermal reservoir rock were assigned a porosity of 0.20, a density of 1500 – 1800 kg/m<sup>3</sup> (except for the boundary domains, where rock density was 2300 kg/m<sup>3</sup> assigned), and a heat conductivity of 1.6 W/m °C. Base rocks were assigned a porosity of 0.02, a density of 2300 – 2800 kg/m<sup>3</sup>, and a head conductivity of 2.1 W/m °C. Specific heat was 1000 kJ/kg °C throughout the model domain.

**Double-Porosity Conversion**

Mid-layer elements were MINC-processed to introduce double-porosity conditions with a fracture spacing of 170 m and a specific fracture volume of 0.3. Domains are renamed as follows:

ROCK1→frac1+matr1, ROCK2→frac2+matr2, and ROCK4→frac4+matr4.

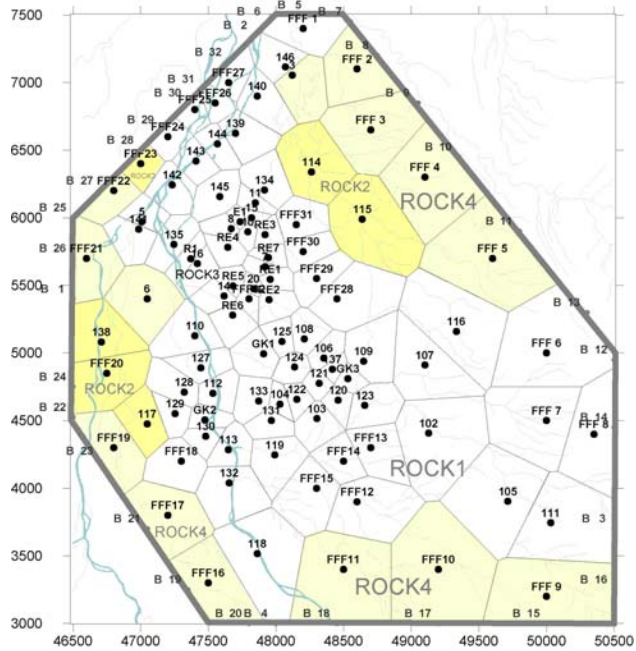


Fig. 2 Mid-layer of the model (-250 m.a.s.l.): hydrothermal reservoir. ROCK1, ROCK2 and ROCK4 are domains with different petrophysical properties. Horizontal boundaries – no flow and no heat transfer conditions.

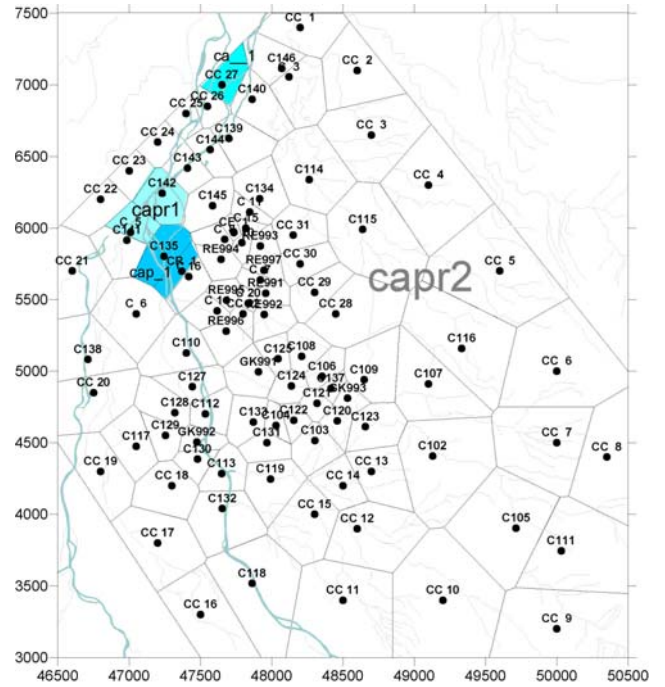


Fig. 3 Upper layer of the model (+100 m.a.s.l.): caprock with three permeable “hydraulic windows”, where natural discharge takes place: capr1, cap\_1, ca\_1.

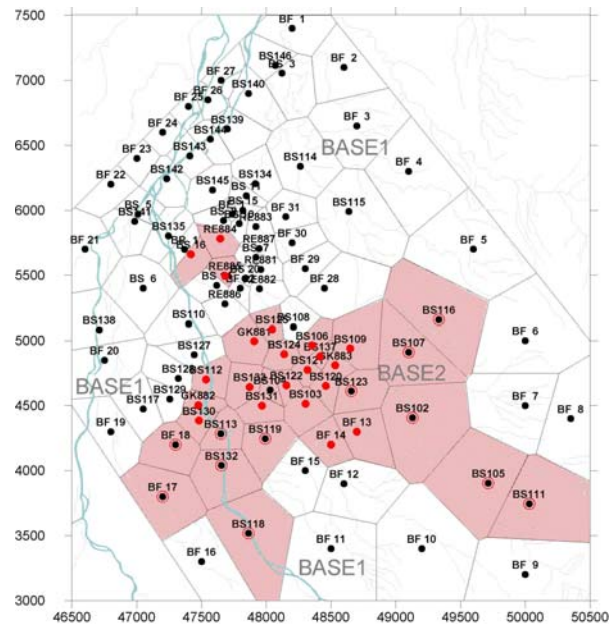


Fig. 4 Base-layer of the model (-750 m.a.s.l.): MASS source elements – red circles (C1,C2 – filled, C1,C4 – open), BASE1 – upflows domain, and BASE2 – host base rock.

## NATURAL STATE MODEL CALIBRATION

### Model Parameterization

Calibration points for natural state modeling include: (1) Vertically averaged temperatures in the mid-layer hydrothermal reservoir (52 T-points); (2) Pressures calculated at -250 m.a.s.l. (based on level and temperature logs in wells) (14 P-points); (3) Natural discharge rates (2 values). Estimated parameters include mass flow rates assigned at the bottom of the base, and the mid-layer hydrothermal reservoir fracture permeability distribution (frac1+frac4, frac2).

### iTOUGH2 Parameter Estimates, Modeled and Observed Data Match, and Sensitivity Analysis

The Levenberg-Marquardt algorithm implemented in iTOUGH2 was used to minimize the weighted least-squares objective function, which is measure of the discrepancy between modeled and observed data at the calibration points. The calibration against temperature data in the central part indicated that it is very unlikely that an open lateral boundary exists.. Therefore, the lateral boundaries were closed, and the following estimates were obtained (run #NS7-4k): permeabilities of 87 mD (frac1, frac4), 20 mD (frac2), a total upflow rate of 40.5 kg/s (including 17.1 kg/s with 950 kJ/kg (C1-sources), 2.8 kg/s with 950 kJ/kg (C3), 9.5 kg/s with 1050 kJ/kg (C2) and 11.1 kg/s with 1050 kJ/kg (C4)). Estimated parameters show low correlation (-0.35), so the range of 95% confidence is reasonably estimated as [62 mD, 107 mD] for permeability, and [35.8 kg/s, 45.3 kg/s] for upflow rate.

Figs. 5 and 6 show the match between the model and measured temperatures and pressures (run #NS7-4k): standard deviation of temperature residuals is 7°C, standard deviation of the pressure residuals is 0.5 bars; the discharge rate was matched to 6% of the observed value. The relatively large pressure deviations are considered acceptable because of the poor quality of the pressure data.

The sensitivity analysis reveals that the temperature data are approximately equally sensitive to both estimated parameters (permeability and upflow rate), with temperatures at points 114, 115, 116, 117, 136 and 138 showing higher sensitivities.

### Comparison of iTOUGH2 and Previous Estimates

We compared the iTOUGH2 estimates with previous assessments by Kiryukhin and Yampolsky (2004). Permeability estimates agree reasonable well with previously obtained values of 100 mD. However, the upflow rate estimated by iTOUGH2 is 40.5 kg/s, which is significantly less than previous estimates of 224 kg/s. This is most likely a result of (1) the change in lateral boundary conditions, (2) the fact that

remote temperature data were not included in the previous, manual calibration, which was restricted to matching the 190°C isotherm only; and (3) the underestimation of heat conductivity (which estimated for dry conditions) may follow a reduced upflow estimate (by 10-15%).

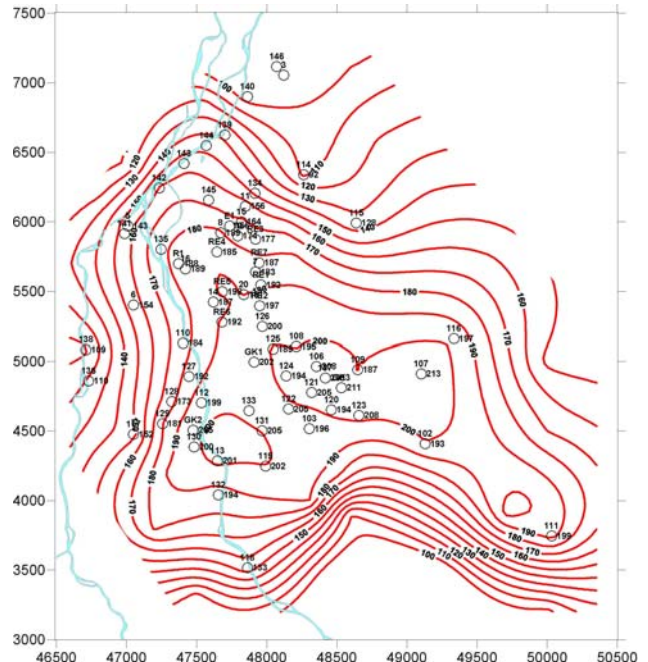


Fig. 5 Natural state modeling temperature distributions vs. observation temperature data.

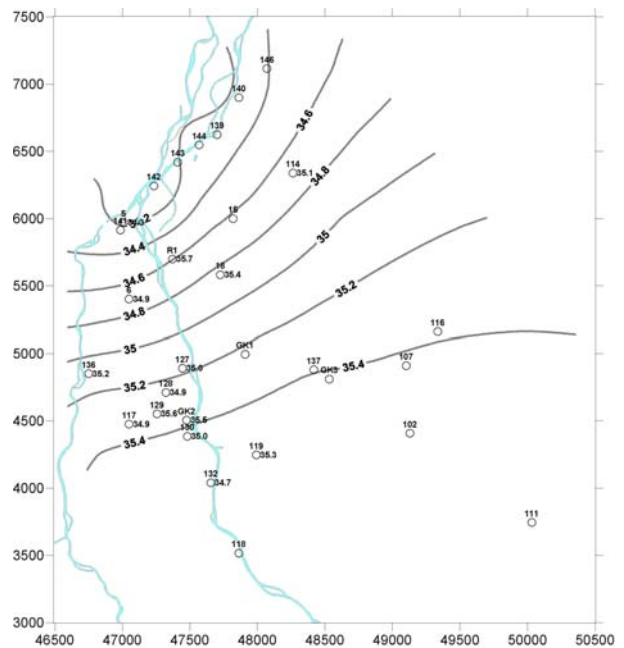


Fig. 6 Natural state modeling pressure distributions vs. pressure data in bars.

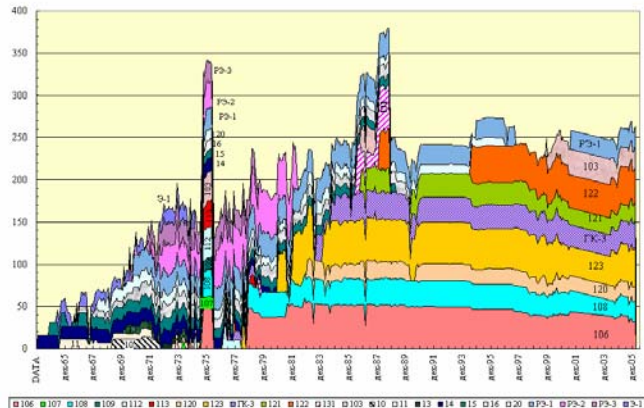
**CALIBRATION OF EXPLOITATION MODEL (1966-2005)**

**Model Parameterization (1)**

Calibration data sets for exploitation modeling include: (1) Monthly averaged enthalpies in exploitation wells (20, RE1, 106, 108, 120, 121, 122, 123, ГК3, 103) (10 E-datasets), (2) monthly averaged pressures at -250 m.a.s.l. (based on level and temperature logs in wells) (24 P-datasets), and (3) monthly averaged temperatures in the mid-layer hydrothermal reservoir (26 T-datasets). The total number of calibration points used was 15,030. Estimated parameters include fracture porosity ( $\phi_f$ ) (domains frac1, frac4), and compressibility ( $C, Pa^{-1}$ ) (frac1, frac4, matr1, matr4, BASE1, BASE2).

**iTOUGH2 Parameter Estimations and Data Match (1)**

Exploitation was modeled by specifying monthly averaged production and reinjection rates (January 1965 – December 2005) (Fig. 7), using the natural state temperature and pressure distribution as initial conditions.



Суммарный расход реинжекционных скважин (закачка холодных и термальных вод).

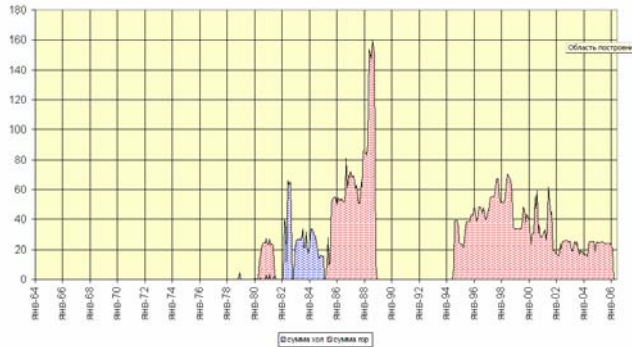


Fig. 7 Extraction (above) and reinjection (below) rates during of exploitation 1965-2005 (N.P. Asaulova data).

It was not possible to reach reasonable agreement between modeled and observed data using the previously estimated parameters; pressures were systematically underestimated, while enthalpies were overestimated.

**Model Parameterization (2)**

Due to the discrepancies suggested that a base porosity value should be added to the inversion to allow for an increased upflow rate in response to exploitation. Moreover, meteoric water infiltration inside of the geothermal field needed to be introduced (see Fig.8). Three additional “hydraulic windows” were introduced in the model’s upper-layer caprock:  $k_N$  (North site caprock permeability),  $k_W$  (West site caprock permeability) and  $k_E$  (East site caprock permeability; see Fig. 9).

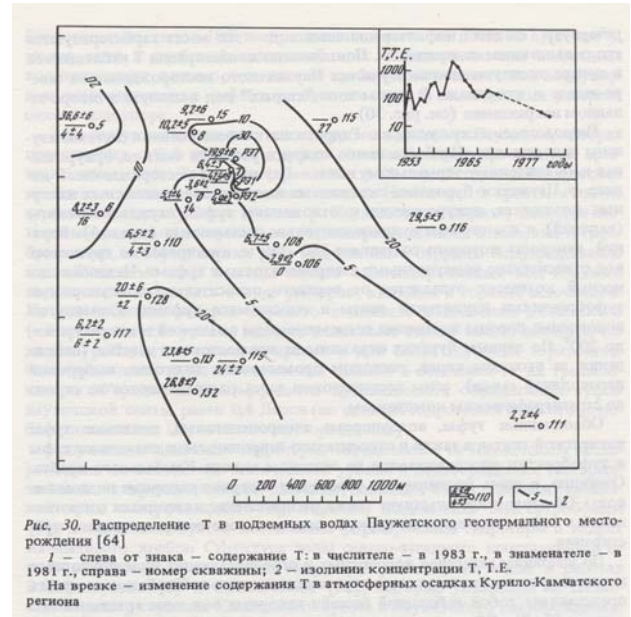


Fig. 8 Tritium distribution in Pauzhetsky field (1981-1983) (Kiryukhin and Sugrovov, 1987) show significant infiltration of cold meteoric waters into hydrothermal reservoir.

**iTOUGH2 Parameter Estimations, Model and Observed Data Match and Sensitivity Analysis (2)**

The following estimates were found (run #7Y6):

Table 1: Parameter Estimates and Their Uncertainties

Estimated parameter	Value	95% confidence interval
$C, Pa^{-1}$	$1.11 \cdot 10^{-6}$	$1.03 \cdot 10^{-6} - 1.21 \cdot 10^{-6}$
$\phi_f$	0.054	0.040-0.068
$k_N, mD$	224	194-258
$k_W, mD$	115	100-132
$k_E, mD$	11	10.1-11.8

Figs. 10-12 (run #7Y6) show modeled and observed data, with the mean residual of enthalpies at the production wells, temperature, and pressure of 41.5 kJ/kg, 15.6°C, and 1.5 bars, respectively. The following measures will likely improve the matches: (1) Recent installations of orifice meters and trays for separate water will yield additional high quality data for production wells, (2) pressure datasets in the central monitoring wells (124, 133, 131) need to be corrected by removing pressure records from wells under wellhead pressures, (3) temperature records need to be corrected, and (4) remove data sets from reinjection wells that are not in equilibrium with reservoir conditions. Additional model improvements may be obtained through more accurate assignment of the infiltration domains.

All calibration data sets are sensitive to changes in the estimated parameters. The most sensitive are the P-datasets from the center wells (124, 131, 133, 129) and E-datasets from wells under cooling conditions (RE1, 106, 20, 108).

The estimated parameters (compressibility, fracture porosity, and “hydraulic windows” permeabilities) were relatively weakly correlated (less than 0.3, and greater -0.7), helping to reduce the estimation uncertainty (see Table 1 above).

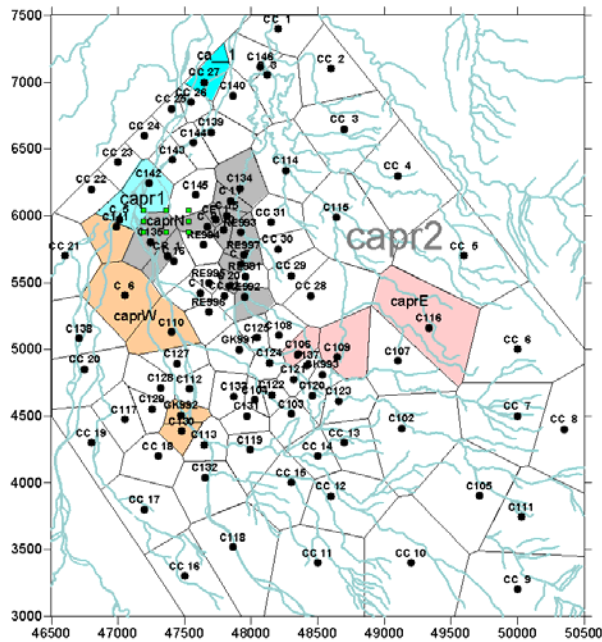


Fig. 9 Revised upper-layer caprock of the model grid (+100 m.a.s.l.): additional permeable “hydraulic windows” added (domains caprN, caprW, and caprE).

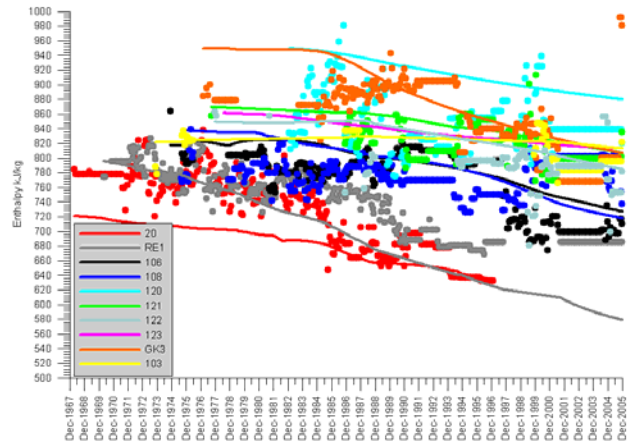


Fig. 10 Modeling enthalpies of exploitation wells (solid lines) vs. observed data (dots).

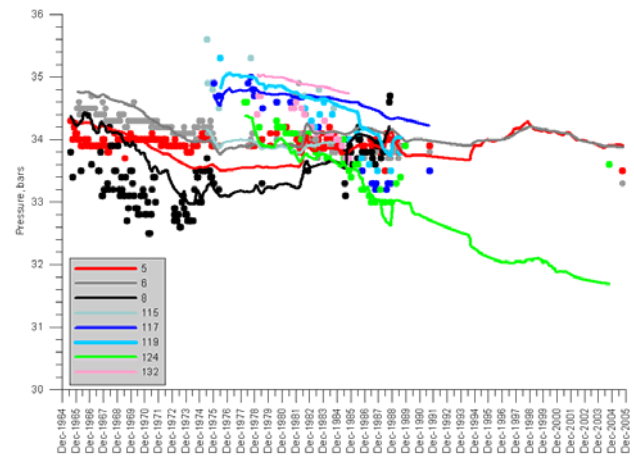


Fig. 11 Modeling pressures (-250 m.a.s.l.) in monitoring wells (solid lines) vs. observed data (dots).

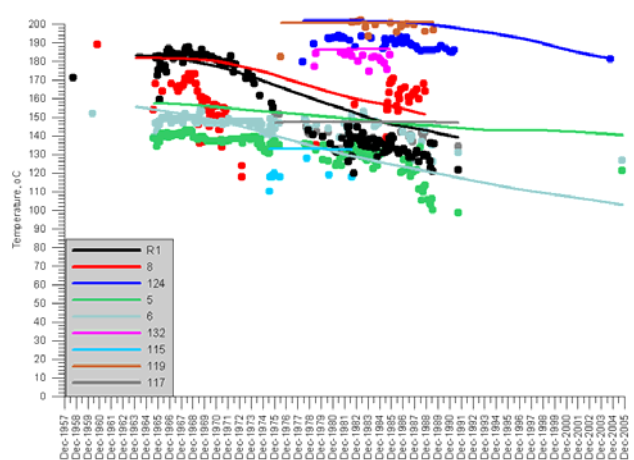


Fig. 12 Modeling temperatures (vertically averaged in hydrothermal reservoir layer) in monitoring wells (solid lines) vs. observed data (dots).

**HEAT, MASS AND CHEMICAL BALANCES OF THE PAUZHETSKY HYDROTHERMAL RESERVOIR**

Heat and mass balances can be derived from the simulations (run #7Y6) to understand sources of exploitation reserves.

The components of the mass flows balance by Nov. 2005 are the following (Fig. 13):

- F1. Natural upflow rate: +40.5 kg/s;
- F2. Additional upflow rate, induced by exploitation: +115.0 kg/s;
- F4. Meteoric water infiltration: +91.3 kg/s;
- F5. Separate reinjection: +23.8 kg/s.
- F6. Hydrothermal reservoir fluid capacity (calculated from balance): +8 kg/s;
- F7. Flow rate from exploitation wells (RE1,103, 106, 108, 120, 121, 122, 123, GK3): -269.3 kg/s;
- F8. Fluid discharge from reservoir: -9.3 kg/s.

The components of the heat flow balance by Nov. 2005 are the following (Fig. 13):

- HF1. Natural upflow: +40.5 MW;
- HF2. Additional heat upflow rate, induced by exploitation: +115.9 MW (3.6 MW +112.3 MW)
- HF3. Conduction heat flow from base rock: +1.7 MW;
- HF4. Meteoric water infiltration: +1.1 MW;
- HF5. Separate reinjection: +12.0 MW;
- HF6. Hydrothermal reservoir heat storage capacity (calculated from balance): +60.5 MW;
- HF7. Heat flow rate from exploitation wells (RE1,103, 106, 108, 120, 121, 122, 123, GK3): -214 MW;
- HF8. Heat discharge from reservoir: -5.2 MW;
- HF9. Conduction heat flow losses through caprock: -12.5 MW.

Chemical balance based on chloride may be calculated, if parental fluid Cl<sup>-</sup> concentration (C1=1600 ppm (Pauzhetka et al., 1965) is assumed to be equal to the additional upflow (induced by exploitation) fluid concentration C2 and to the reservoir fluid chloride concentration C3, so that C1=C2=C3=1600 kg/kg; meteoric chloride concentration C4=10 ppm; the chloride concentration of the reinjected water is C5, and the remaining springs discharge chloride concentrations C8 are assumed to be C5=C8=1300 ppm.

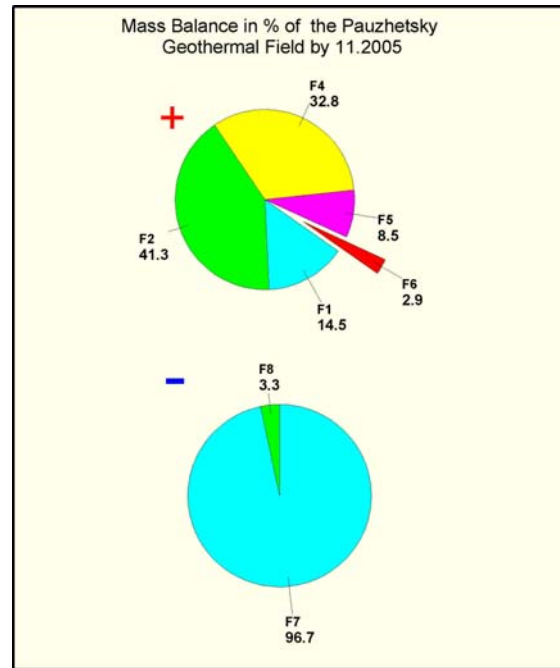


Fig. 13 Mass balance of the Pauzhetsky hydrothermal reservoir (run #7Y6). Positive and negative balance components are shown on the upper and lower graphs, respectively; Flux contributions F# are explained in the text.

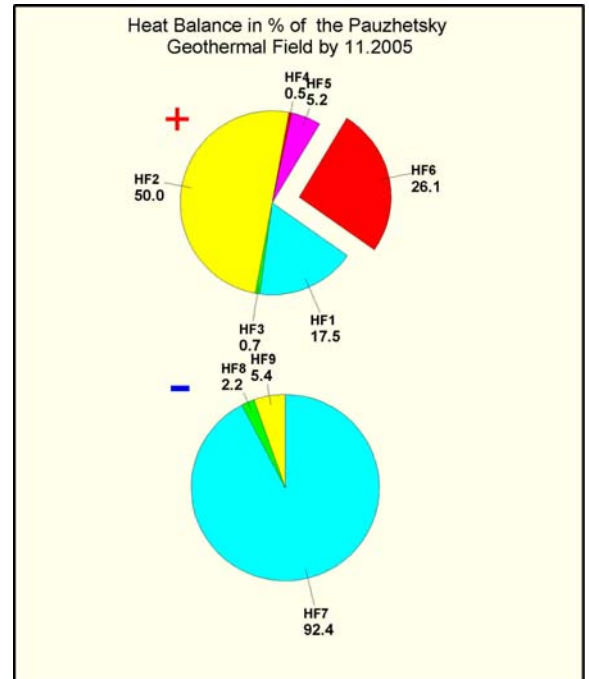


Fig. 14 Heat balance of the Pauzhetsky hydrothermal reservoir (run #7Y6). Positive and negative balance components are shown on the upper and lower graphs, respectively. Heat flow components HF# are explained in the text

Based on mass balances above, the following chloride mass flows derived:

CF1. Chloride natural upflow rate:

$$CF1 = +F1 * C1 = +65 \text{ g/s.}$$

CF2. Additional chloride upflow rate, induced by exploitation:  $CF2 = +F2 * C2 = +184 \text{ g/s.}$

CF4. Meteoric water chloride infiltration:

$$CF4 = +F4 * C4 = +1 \text{ g/s.}$$

CF5. Chloride in separate reinjection:  $CF5 = +F5 * C5 = +31 \text{ g/s.}$

CF6. Chloride from hydrothermal reservoir fluid capacity:  $CF6 = +F6 * C6 = +13 \text{ g/s.}$

CF8. Chloride discharge from reservoir:

$$CF8 = -C8 * F8 = -12 \text{ g/s.}$$

Hence, chloride mass flow from exploitation wells CF7 (chloride mass flow from exploitation wells) can be estimated as:

$$CF7 = CF1 + CF2 + CF3 + CF4 + CF5 + CF6 + CF8 = 282 \text{ g/s.}$$

Actual chloride mass flow from exploitation wells (RE1,103, 106, 108, 120, 121, 122, 123, GK3) are estimated based on a chemical analysis of extracted fluids and well flowrates as 260-271 g/s, which are within 4-8% of the previous estimates, confirming model calibration results.

## CONCLUSIONS

(1) The Pauzhetsky geothermal reservoir was represented in the model as a three-layer system of the existing well field. This model includes: (1) Mid-layer hydrothermal reservoir at -250 m.a.s.l. with an average thickness of 500 m; (2) Upper layer caprock with "hydraulic windows" representing natural discharge zones; (3) Base layer with the upflow zone of an average thickness of 500 m.

(2) For the iTOUGH2 natural state modeling, calibration data include 68 points (2 natural discharge rates, 14 reservoir pressures at -250 m.a.s.l., 52 reservoir vertically averaged temperatures). The different quality of the calibration points was expressed by specifying appropriate standard deviations. Estimates of the following parameters were obtained: (1) permeability, and (2) upflow rate.

(3) For the modeling of the exploitation phase using iTOUGH2, calibration data include 60 datasets: enthalpies of the exploitation wells (10 data sets), pressures in monitoring wells (24 data sets), and temperatures in monitoring wells (26 data sets), for a total of 15,030 calibration records. Preliminary

estimation of the following principal parameters was performed: (1) reservoir compressibility (needed to estimate additional upflow induced by exploitation), (2) reservoir fracture porosity (as an effective reservoir heat extraction parameter defining the active volume of the hydrothermal reservoir), (3) permeabilities of infiltration windows. Heat and mass balances derived from the model are used to understand the sources of exploitation reserves. Chemical balances were calculated to corroborate the calibration results.

(4) Model calibration is still on going and will be followed by an analysis of the sustainable capacity of the Pauzhetsky field.

## ACKNOWLEDGMENT

This work was supported by SUE "Kamchatskburgeotermia", FEB RAS project 06-I-OH3-109 and RFBR project 06-05-64688-a.

## REFERENCES

Kiryukhin, A.V., Sugrobov, V.M., *Heat and Mass Transfer in Hydrothermal Systems of Kamchatka*, Moscow, Nauka publ., 1987 (in Russian).

Kiryukhin, A.V., V.A. Yampolsky Modeling Study of the Pauzhetsky Geothermal Field, Kamchatka, Russia, *Geothermics*, 33(4), 421-442, 2004.

*Pauzhetka Hot Springs in Kamchatka*, B.I.Piip editor, Moscow, Nauka publ., 1965. (in Russian).

Pruess, K., C. Oldenburg, and G. Moridis, *TOUGH2 User's Guide, Version 2.0*, Report LBNL-43134, Lawrence Berkeley National Laboratory, Berkeley, Calif., 1999.

Finsterle, S., *iTOUGH2 User's Guide*, Report LBNL-40040, Lawrence Berkeley National Laboratory, Berkeley, Calif., 1999.

Finsterle, S., *iTOUGH2 Command Reference*, Report LBNL-40041, Lawrence Berkeley National Laboratory, Berkeley, Calif., 1999.

Finsterle, S., *iTOUGH2 Sample Problems*, Report LBNL-40042, Lawrence Berkeley National Laboratory, Berkeley, Calif., 1999.